ISSN: 2414-1895 DOI: 10.6919/ICJE.202412_10(12).0013

Force Equalization Control of Redundant Electromechanical Actuation System based on Fractional Order Controller

Dong Hou[1, a], Jianzhong Yang[2, b], Xiaozhe Sun[2, c], Cheng Yuan[3, d], Chenguang Yang[4, e]

[1] China Aerospace Science and Industry Corporation Third Research Institute 304 Research Institute, Beijing 100744, China

[2] College of Safety Science and Engineering, Civil Aviation University of China, Tianjin 300300, China

[3] Nanjing Les Information Technology Co., Ltd., Nanjing, China

[4] Tianjin Sub-bureau of North China Regional Air Traffic Management Bureau, CAAC, Tianjin, China

[a]18344651516@163.com, [b]jzyang2004@126.com, [c]sxz_2002@163.com, [d]1192897930@qq.com, [e]869298395@qq.com.

Abstract

To address the force fight problem in the fly-by-wire redundant actuation system, which poses risks to system safety during the position response process of the active-active dual redundant electromechanical actuation systems (EMAs), a feedback force equalization control method is proposed. This method targets the shortcomings of the traditional PID controller, which is characterized by poor stability and a tendency for overshoot. Instead, an optimized Fractional Order PID (FOPID) controller is adopted . This method takes the output deviation of force difference and position error of two electromechanical actuators as input, and the FOPID generates position compensation signal, so as to achieve the optimization goal of reducing force fight and improving system position response performance, Aiming at the limitation of traditional parameter tuning, the controller parameters are optimized iteratively using particle swarm optimization (PSO) algorithm. Under the command of step response and triangle wave with the maximum deflection angle of the rudder surface, by setting a serious force fight situation under the joint action of multiple disturbances to compare the control effect of PID method and FOPID method of PSO algorithm on force fight and position response, the experimental results show that FOPID can control static force fight and dynamic force fight several times more effectively than traditional PID; It can effectively improve the impact of force fight on the system.

Keywords

Redundant Actuator System; Electromechanical Actuators; Force Fight; Fractional Order Controller; Particle Swarm Optimization; Force Equalization.

1. Introduction

With the development of multi-electric aircraft in the aviation sector, an increasing number of flight control systems are utilizing electromechanical actuators as their primary driving components. One of the critical challenges in the control systems of multi-electric aircraft is the development of a high-

ISSN: 2414-1895 DOI: 10.6919/ICJE.202412_10(12).0013

performance and safe electromechanical actuation system [1,2].To meet the safety requirements of flight control systems, modern civil aircraft control surfaces are typically equipped with a redundant architecture comprising two or more actuators, which operate in an active-active redundant mode to jointly drive the control surfaces [3]. There is a significant problem with the dual redundant electromechanical actuation system (EMAs)operating in active-active mode: due to the high stiffness, strong coupling, and nonlinearity of the electromechanical actuation system, the dynamic position response of the two actuators are different, and there is always a phenomenon of unbalanced output torque, that is, force fight. Force fight can have adverse effects on the control surface structure and system power. Long term uneven force fight may lead to material cracking and fatigue, reduce system load ability, and even have a serious impact on flight safety.

1.1 Research Status of Force Fight

At present, the primary control methods for mitigating force fight include structural compensation and the introduction of force feedback signals for compensation [4-8]. Numerous researchers have designed control loops to address this issue. In 2014, Zhang [9] from Xi'an University of Technology proposed a PID feedback method to compensate for position signals, which significantly reduced force fight during the dynamic response process. In 2019, Salman et al. [10,11] from Beihang University applied linear matrix inequalities (LMIs) to design disturbance observers and controllers for the force fight problem in non-similar redundancy actuation systems. They demonstrated effective control over external load disturbance signals; however, the state observer could only compensate for a limited number of observable disturbances. In 2020, Xue et al. [12] from Shanghai Jiao Tong University introduced a force equalization algorithm based on pressure differences and position compensation feedback. In 2021, Wu Rehman et al. [13] from Beijing University of Science and Technology designed a fractional-order PID feedback controller based on a linear simulation model of dissimilar redundant systems, but they only verified the force fight response under external load disturbances. The control methods discussed in these studies have, to some extent, reduced force fight during dynamic response procedures. However, when designing control algorithms or assessing the anti-interference performance of these algorithms, the focus has primarily been on force fight caused by external load changes, with insufficient attention given to the impact of system parameter perturbations. Furthermore, the approach of manually adjusting controller parameters using classical theory to derive control parameters may not necessarily yield optimal results.

In order to enhance the stability and control accuracy of PID force equalization controllers, this paper addresses the control requirements for minimizing force fight while also considering the accuracy of the system's position response. A fractional-order force equalization feedback control method is developed, and a particle swarm optimization algorithm [14] is employed to optimize the controller parameters, thereby achieving optimal control performance.

2. Modeling and Simulation of Electromechanical Actuation System

2.1 Working Principle of EMAs

2.1.1 Block Diagram of EMAs

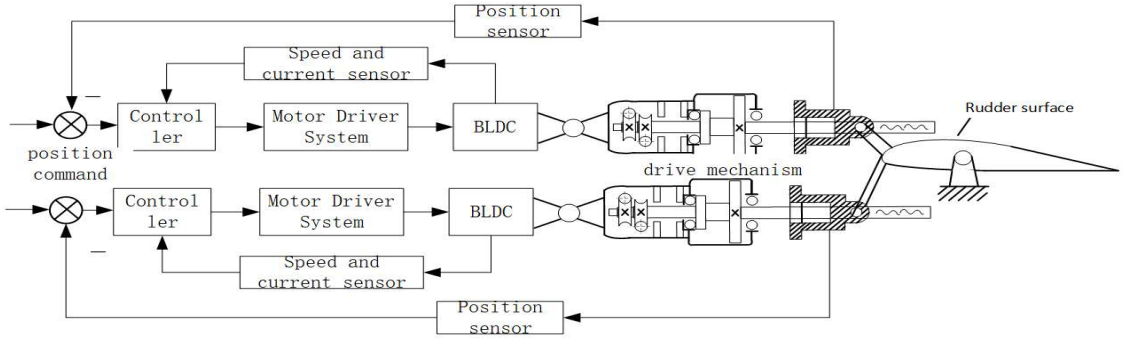

Figure 1. Double redundant EMAs platform

ISSN: 2414-1895 DOI: 10.6919/ICJE.202412_10(12).0013

The schematic diagram of the dual redundant electromechanical actuation system is illustrated in Figure 1, where the output forces of the two actuators collectively act on the rudder surface. The position sensor measures the actual deflection angle of the control surface for comparison. The controller generates a position signal to drive the BLDC motor, which produces the output displacement; this output displacement, in turn, drives the rudder deflection.

2.1.2 Formula Calculation of EMAs

In an ideal scenario, where the magnetic resistance of the rotor remains constant regardless of its position and the three-phase windings are symmetrical, the balance equation for the stator voltage of a Brushless Direct Current (BLDC) motor can be expressed as the following state equation(1). u_a、u_b、u_c represents phase voltage (V), i_a、i_b、i_c represents phase current (A), e_a、e_b、e_c represents winding back electromotive force (V), R represents phase resistance(Ω), L and M represent winding inductance and winding mutual inductance (H), respectively:

$$\begin{bmatrix} u_a \\ u_b \\ u_c \end{bmatrix} = \begin{bmatrix} R & 0 & 0 \\ 0 & R & 0 \\ 0 & 0 & R \end{bmatrix} \begin{bmatrix} i_a \\ i_b \\ i_c \end{bmatrix} + \begin{bmatrix} L-M & 0 & 0 \\ 0 & L-M & 0 \\ 0 & 0 & L-M \end{bmatrix} P \begin{bmatrix} i_a \\ i_b \\ i_c \end{bmatrix} + \begin{bmatrix} e_a \\ e_b \\ e_c \end{bmatrix} \tag{1}$$

Equation (1) obtains the relationship between the internal voltage and current of the motor through three-phase equivalent transformation, as shown in Equation (2). Ra and La are the equivalent resistance and inductance, respectively, K_e is the back electromotive force constant.

$$U_d = 2RI + 2(L-M)\frac{di}{dt} + 2e_d = R_a I + L_a \frac{di}{dt} + k_e \omega \tag{2}$$

The electromagnetic torque equation of brushless DC motor:

$$T_e = (e_a i_a + e_b i_b + e_c i_c) / \omega \tag{3}$$

The motion equation of BLDC is shown in equation (4), where B is the damping coefficient (N · m · s/rad). J is the moment of inertia of the motor (kg·m2), T_l is the load torque (N · m), and T_f is the friction torque (N · m).

$$T_e = T_l + T_f + B\omega + J\frac{d\omega}{dt} \tag{4}$$

During the operation of civil aircraft systems, they will be subjected to flight loads. The control surface is equivalent to an inertial load system as shown in equations (5) and (6). x_a represents the linear output displacement of the ball screw, x_L represents the deflection displacement of the rudder tail (m), represents the rudder mass (kg), represents the rudder damping coefficient (N/(m/s)), represents the rudder stiffness coefficient, represents the motor output driving force, and M_{cs} represents the connection stiffness. The relationship between the deflection angle of the control surface θ and the deflection displacement of the control surface x_L can be equivalent to a

ISSN: 2414-1895 DOI: 10.6919/ICJE.202412_10(12).0013

proportional relationship, with the proportionality coefficient being the radius of rotation of the control surface R_{cs} [15].

$$F_i = M_{cs}\ddot{x}_L + B_{cs}\dot{x}_L + K_d x_L \tag{5}$$

$$F_i = K_{ms}(x_a - x_L) \tag{6}$$

The frequency domain response characteristics of the system are analyzed as shown in Figure 2, with an amplitude margin of 38.1dB and a phase margin of 90.2 °, indicating that the system is a stable system.

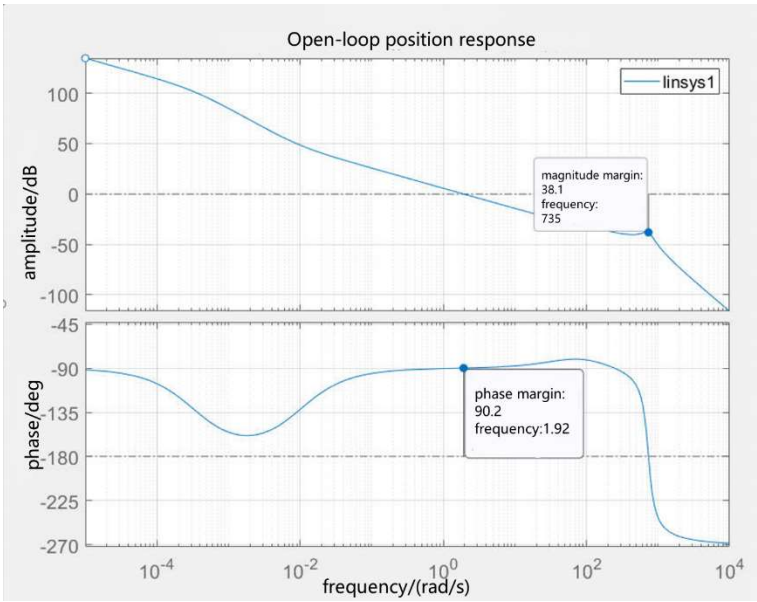

Figure 2. Frequency Domain Characteristics of EMAs

2.2 Analysis of Force Fight

Obtain the force fight as shown in equation (7), $\triangle F_d$ represents the uncertain terms that cause force fight during the operation of the flight control system, such as transmission clearance, transmission device friction, signal transmission circuit delay, noise, etc.

$$F_{ff} = K_{ms1}(x_{a1} - x_L) + K_{ms2}(x_{a2} - x_L) + \Delta F_d \tag{7}$$

The difference in output displacement between two actuators is the main cause of system force fight [16], and the factors that have the greatest impact on force fight in EMAss are shown in Table 1.

By incorporating the aforementioned factors into the dual redundancy electromechanical actuator, the worst-case force contention scenario may arise within the system. Dynamic force fight is defined as the force fight generated during the system's dynamic process before it reaches a steady state, while static force fight refers to the force fight that persists in the system after the position response has stabilized. In this project, the goal is to minimize force contention during system operation, with the peak value of dynamic force fight and the final value of static force contention serving as evaluation indicators. Due to the influence of various uncertain parameters, the dynamic force fight can reach 145,961 N, while the static force fight is approximately 52,561 N.

ISSN: 2414-1895 DOI: 10.6919/ICJE.202412_10(12).0013

Table 1. parameters that affect force fight

Number	Name	Model Representation Form
1	Position signal bias	Increase the input position command to a single actuator by 2% in 0.4s
2	Position command delay	Increase the position command delay signal to a single actuator by 20%
3	Intermittent position signal	The position signal of a single actuator has a 0.01s interruption in 0.2s
4	Noise	The transmission mechanism has a 50hz noise with an amplitude of 0.2% of the position signal
5	Friction	There is a 30% difference in friction between the motor transmission parts
6	Transmission clearance	Increase the clearance of the gearbox of a single actuator by 200%
7	Transmission stiffness difference	Increasing the transmission stiffness of a single actuator by 25%
8	Transmission efficiency difference	reduces the transmission efficiency of a single actuator by 15%
9	Load torque difference	Increase the load torque of a single actuator by 5000N in 0.1s

2.3 The Force Equalization Control Effect of PID Controller

The force fight before and after the implementation of the force equalization PID controller are compared, as illustrated in Figure 3. After incorporating proportional feedback, the peak value of force fight significantly decreased from 148,715 N to 61,204 N. To address the static force fight issue that cannot be fully mitigated by proportional feedback alone, an integral component was added to the feedback loop. The differential control aspect reflects the rate of change of the deviation, which helps to minimize overshoot. Following the addition of the differential element, static force fight are reduced. Overall, the PID controller has effectively improved both static and dynamic force fight.

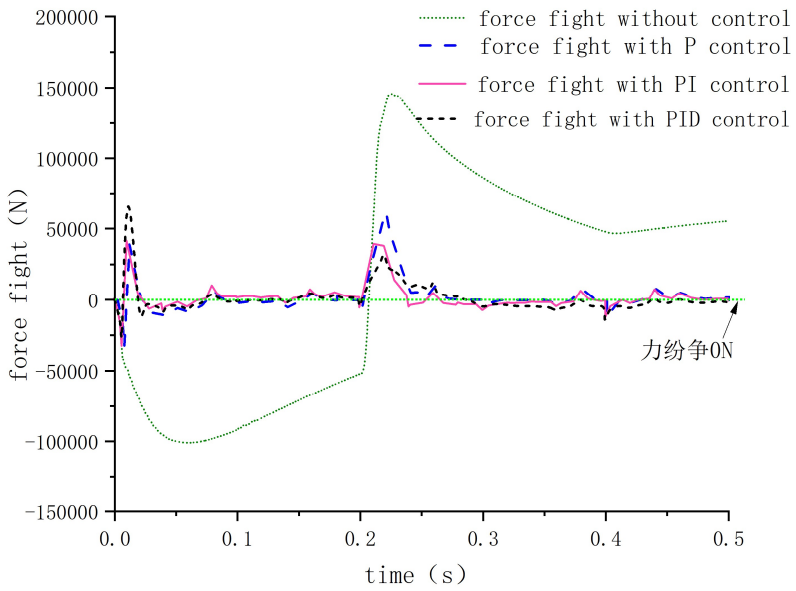

Figure 3. Force Fight Response Before and After Adding PID

ISSN: 2414-1895 DOI: 10.6919/ICJE.202412_10(12).0013

The PID feedback controller features a straightforward structure and effectively mitigates most instances of force fight, but there are some problems such as poor anti-interference ability and suboptimal control performance in dynamic force fight. To address these issues, the PID controller has been optimized.

3. Design of FOPID Controller Parameter Optimized by PSO

This chapter introduces the principle of FOPID control, FOPID parameters using the Particle Swarm Optimization algorithm, and examines the force fight under various parameter groups. It concludes by presenting a set of FOPID force equalization controllers with optimal parameters.

3.1 Design of Fractional Order PID Controller

3.1.1 Definition and Implementation of Fractional Calculus

In order to better explain the mathematical meaning of fractional calculus, an operator of fractional calculus ${}_{t0}\vartheta_t^{\alpha}$ is introduced as shown in equation (8), where α is limited to real numbers and t is the independent variable [17].

$$ {}_{t0}\vartheta_t^{\alpha} f(t) = \begin{cases} \frac{d^{\alpha}}{dt^{\alpha}} f(t), \alpha > 0 \\ f(t), \alpha = 0 \\ \int_t^{t_0} f(\tau) d\tau^{-\alpha}, \alpha < 0 \end{cases} \tag{8} $$

The block diagram of the fractional-order PID control system is illustrated in Figure 4. The fractional-order PID controller extends the concept of integer-order control to the fractional domain by introducing two adjustable parameters: the integral order and the derivative order. The integral order signifies the strength of the integral effect, and selecting an appropriate fractional order can enhance the low-frequency bandwidth while minimizing overshoot in the amplitude frequency characteristics of the control system. A suitable integration order leads to reduced steady-state errors, improved dynamic response accuracy, and enhanced intermediate frequency bandwidth in the system's amplitude frequency characteristics. Implementing a fractional-order PID controller in the force fight control process is advantageous for increasing the controller's responsiveness, decreasing the instantaneous peak value of the force pulse generated by the system during the response phase, and mitigating static force fight. This approach also reduces the steady-state error of the force fight and enhances the overall stability of the system.

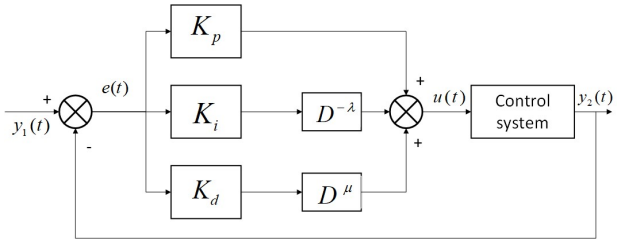

Figure 4. Fractional Order PID Controller Diagram

In practical physical systems, it is necessary to discretize fractional calculus operators[18].

Convert the fractional calculus transfer function into an approximate model of a high-order integer order system using the Oustaloup filter.

3.1.2 Performance Indicators of FOPID Controller Parameters

The smaller the error signal e (t) in the system, the better the performance, as the control signal typically represents energy consumption. Since the error signal e (t) is dynamic, the integral

ISSN: 2414-1895 DOI: 10.6919/ICJE.202412_10(12).0013

performance index is often employed to minimize force fight during system operation. A commonly used evaluation metric for optimal controllers is the time-weighted integral absolute error (ITAE) metric. The ITAE performance metric assigns greater weight to errors over time, meaning that as time increases, the weight of the error also increases. This forces the error signal to converge to zero as quickly as possible, making it particularly suitable for practical servo controller design. The ITAE error integration criterion is defined as: $\int_0^\infty t|e(t)|dt$

Due to the influence of parameter variations and external disturbances, the system experiences significant force fight, and force fight is introduced into the feedback loop to compensate for the dynamic response of the system, these force fluctuations are incorporated into the feedback loop. The performance index of the controller is defined as a composite time integration index that considers both the position response and the magnitude of the force fight. The specific formula for this index is presented in Equation 9, where the weight coefficient is represented, and the parameter weight is allocated according to the parameter magnitude $w_1 = 1\times10^6$, $w_2 = 1$.

$$f(k) = w_1 \int_0^t (|x_a - x_1| + |x_a - x_2|) \cdot tdt + w_2 \int_0^t |F_s - F_m| \cdot tdt \tag{9}$$

The essence of force equalization control is to minimize the difference of output force between actuators. This force difference is primarily associated with the deviation in position response. Therefore, it is essential to design a position synchronization control method [19,20] to achieve the goal of balancing force fight and mitigating related uncertainties and external disturbances within the system. The block diagram for the force equalization feedback control of the dual redundant actuator is illustrated in Figure 5.

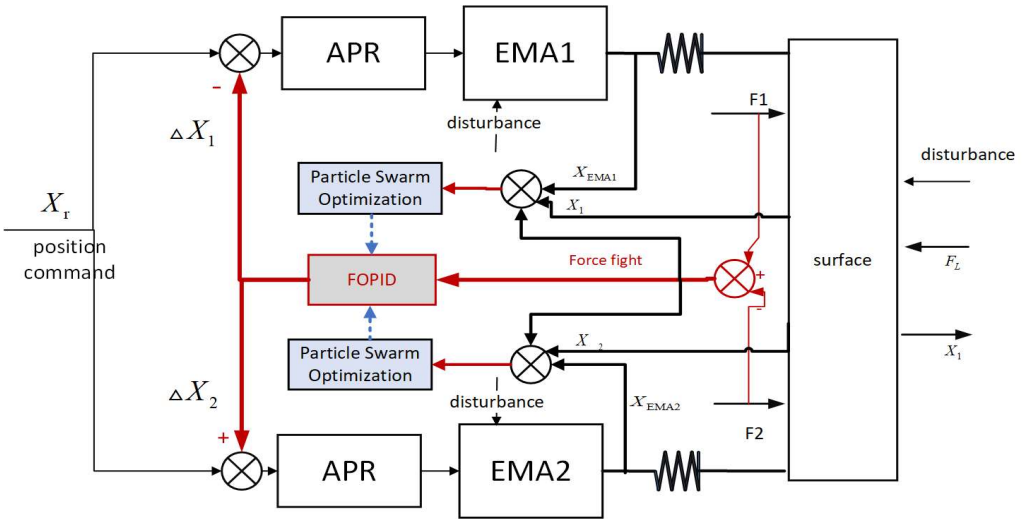

Figure 5. FOPID controller Parameter optimized by PSO

The synchronization signal error and tracking error signal of the two motors are utilized as input variables for optimizing the performance indicators of the controller design, effectively reducing both synchronization and tracking errors simultaneously.

3.2 Parameter Optimization of Particle Swarm Optimization Algorithm

3.2.1 Principle of Particle Swarm Parameter Optimization

The particle swarm optimization algorithm has been chosen as the optimization method for the system force equalization controller [21]. The particle swarm is initialized as a collection of random particles,

ISSN: 2414-1895 DOI: 10.6919/ICJE.202412_10(12).0013

and in each iteration, the particles continuously update based on individual and global extrema to produce a new generation of the population. The control diagram is illustrated in Figure 6.

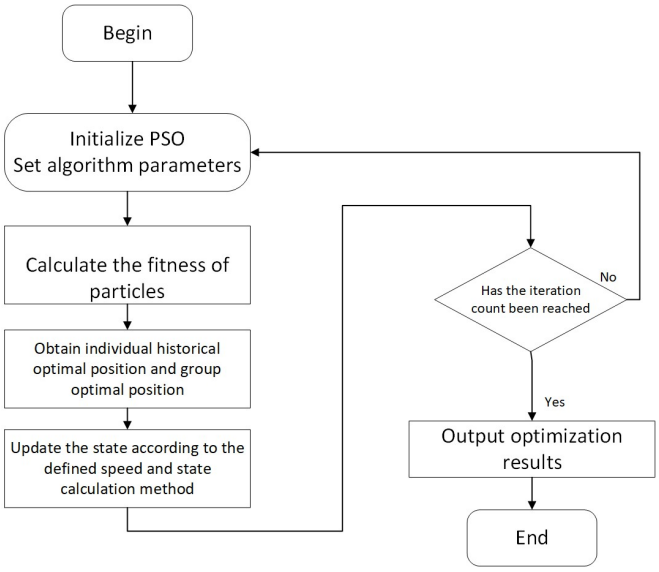

Figure 6. Parameter optimization chart of PSO

In n-dimensional space, define the i-th particle in the particle swarm, $x^i(k)=[x_1^i \quad x_2^i \quad \ldots \quad x_n^i]^T$ represents the current position of the particle. $p^i(k)=[p_1^i \quad p_2^i \quad \ldots \quad p_n^i]^T$ indicates that the particle already has the optimal fitness $f_p^i(k)$. The optimal position of group particles is denoted as $p^g(k)=[p_1^g \quad p_2^g \quad \ldots \quad p_n^g]^T$. $v^i(k)=[v_1^i \quad v_2^i \quad \ldots \quad v_n^i]^T$ represents the search direction of the particle. The speed update and position update formulas of the basic PSO algorithm can be expressed as equation (10).

$$\begin{cases} x_j^i(k+1)=x_j^i(k)+v_j^i(k+1) \\ v_j^i(k+1)=\omega(k)v_j^i(k)+\varphi_1 rand(0,a_1)(p_j^i(k)-x_j^i(k))+\varphi_2 rand(0,a_2)(p_j^g(k)-x_j^i(k)) \end{cases} \tag{10}$$

Among them, $i=1,2,\cdots,m;\quad j=1,2,\cdots,n$, ω is the inertia weight factor, φ_1, $\varphi_2 \in [0,+\infty)$ is the acceleration constant, which controls the learning rate of the relative contributions of individual cognitive components and group social components. $rand(0,a_1)$ and $rand(0,a_2)$ are uniformly distributed random numbers within the range of values, while a_1 and a_2 are the corresponding control coefficients. The first part of the velocity update function is the velocity of the particles at the previous moment; The second part represents the cognitive ability of particles by comparing their current positions with the optimal positions they have experienced before; The third part represents information sharing between particles. To prevent excessive particle velocity, the threshold for velocity is set to $v_{\max}$.

3.2.2 FOPID Parameters Obtained from Particle Swarm Optimization Algorithm

Firstly, initialize the system by setting parameter ranges, including the optimization parameter dimension, inertia factor, particle swarm size, acceleration constant, number of iterations, maximum velocity, and randomly generating the initial position matrix $[x_1,x_2,x_3,x_4,x_5]=[K_P,K_I,K_D,\lambda,\mu]$ along with the initial velocity of the system within the specified value range. Assign the initial parameters of the particles to the controller, run the system simulation model, and calculate the performance

ISSN: 2414-1895 DOI: 10.6919/ICJE.202412_10(12).0013

output indicators during each iteration. Continuously update the position and velocity of the particles based on the iterative performance indicators until the optimal parameter combination for the system is achieved. The optimal fitness value reflects the degree of conformity of the indicator function; a smaller fitness value indicates a smaller error in the indicator function. In other words, as the number of iterations increases, the system parameters are gradually optimized, resulting in a decrease in the optimal fitness value. As the number of iterations increases, the fitness value exhibits a trapezoidal downward trend. The iterative process and the optimal individual fitness values for each generation are illustrated in Figure 7.

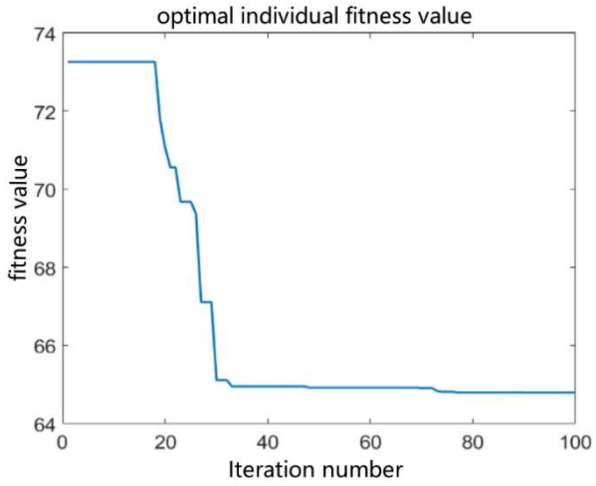

Figure 7. Optimal individual fitness curve

According to the parameter range selected by the feedback PID controller, establish the upper and lower bounds for the proportional (P), integral (I), and derivative (D) parameters based on empirical values. Due to the random generation of initial parameters and velocities in the particle swarm optimization algorithm, the optimized parameters obtained in each iteration may vary [22]. A binary method from mathematics is employed to continuously adjust the boundary conditions of these parameters. The typical range of order values for general fractional calculus is (0, 1); however, experience indicates that excessively high orders can diminish system stability, while low orders may lead to inadequate control flexibility. Controllers with order values between (0.4, 0.7) tend to exhibit relatively stable control effects. Each optimization iteration is conducted 100 times, and the range of boundary conditions is adjusted appropriately based on the parameter results after each optimization. The optimized parameters and their corresponding ITAE index values for five different boundary conditions are presented in Table 2.

Table 2. Combination of optimization parameters under different boundary conditions

Parameters /Groups	P	I	D	λ	μ	ITAE
1	8.14E-6	8.0E-7	1.0E-9	1.2852	0.9165	95.45
2	9.34E-6	9.96E-7	9.69E-9	0.4813	0.5119	95.55
3	9.50E-6	1.00E-6	1.00E-8	0.4814	0.5289	101.72
4	1.50E-5	1.57E-6	8.59E-8	0.5	0.5065	86.21
5	1.96E-5	1.24E-6	7.03E-8	0.4540	0.5002	65.62

ISSN: 2414-1895 DOI: 10.6919/ICJE.202412_10(12).0013

Taking the fifth group as an example, the ranges of P, I, and D are respectively taken, and the ranges of integral and differential orders are (0.45, 0.5), and (0.5, 0.55). P. The iterative optimization curves of parameters I and D, as well as the optimization curves of fractional order parameters, are shown in Figure 8.

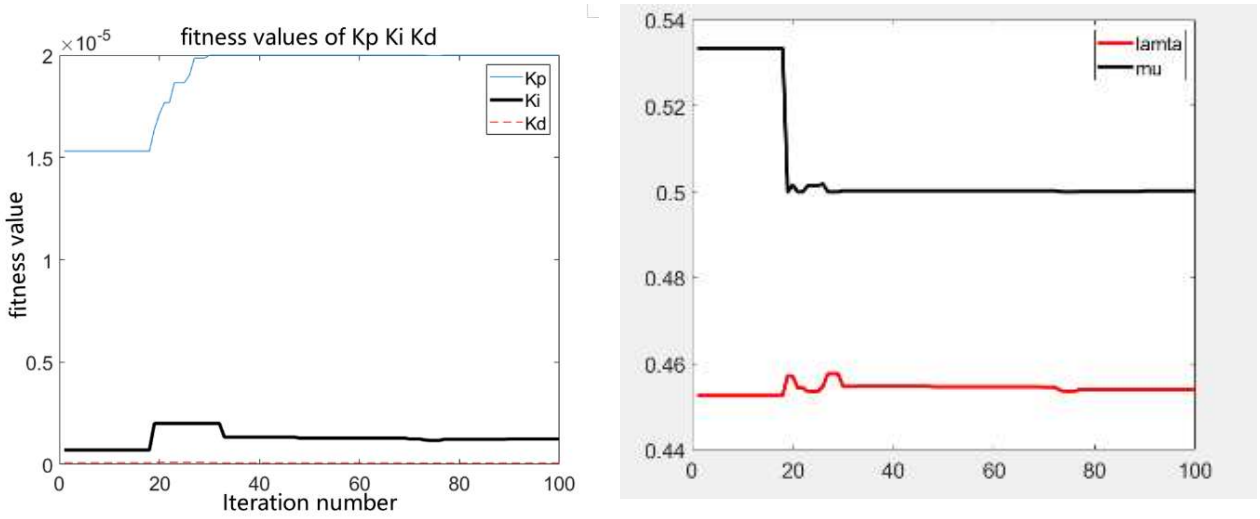

(a)Optimization curve of PID (b) Optimization curve of fractional order

Figure 8. Parameter Optimization Curve

Comparing the system force fight and position response under the above five sets of controller parameters, as shown in Figure 9, it can be seen that the dynamic force fight under the fifth set of parameters is the smallest, and the static difference of position response is small. Choose P=1.957E-5, I=1.24E-6, D=03E-8, $\lambda = 0.45402$, $\mu = 0.50019$, As the optimal parameter for FOPID controller.

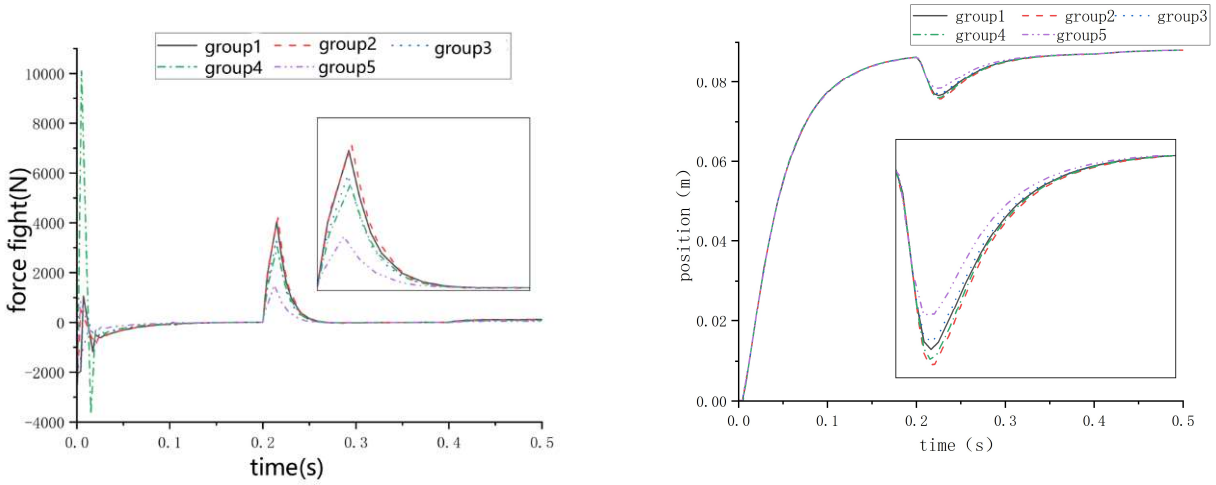

(a)Force fight Response (b)Step signal response

Figure 9. System response under different parameters

3.3 Control System Effect and Analysis

3.3.1 Verification of Step Response Control Effect

To evaluate the effectiveness of the fractional-order PID controller on force fight, we compared the response of the integer-order PID controller with that of the system after implementing the fractional-

ISSN: 2414-1895 DOI: 10.6919/ICJE.202412_10(12).0013

order PID controller, as illustrated in Figure 10. Qualitatively, the introduction of the fractional-order PID controller significantly enhances the peak value of dynamic force fight and reduces static force fight to below 100 N.

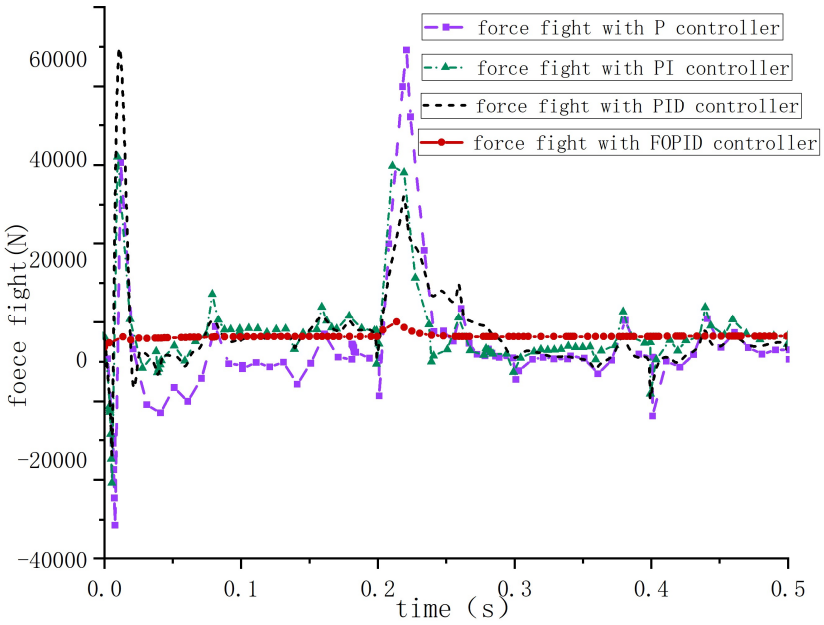

Figure 10. Comparison of force fight under different controllers

Statistical analysis of the maximum dynamic force fight and static force fight in the system response process under different control methods is shown in Table 3. PID controller can control the maximum force fight within 19% of the original force fight, and FOPID can control the maximum force fight within 2.3% of the original. The PID controller controls the static force fight within the original 7%, while FOPID controls the static force fight within 0.08%. The control effect of dynamic force fight increased by 87.9%, and the control effect of static force fight increased by 96 times.

Table 3. Controller performance comparison

Controller	Maximum force fight	Static force fight
None	145861N	52561N
P	61610N	7630N
PI	38847N	4372N
PID	27523N	3596N
FOPID	3308N	37N

In addition, a comparison of the position step response performance of the system under different controllers is shown in Figure 11.

It can be seen that after adding force balancing PID control, the maximum static error of the system at 0.2 seconds increased from 9.03% to 14.6%. This is due to the introduction of a force feedback loop, which increases the delay of the system and reduces its speed. After introducing FOPID feedback, due to its flexibility in frequency response, the static position error has been improved by about 11.86%.

ISSN: 2414-1895 DOI: 10.6919/ICJE.202412_10(12).0013

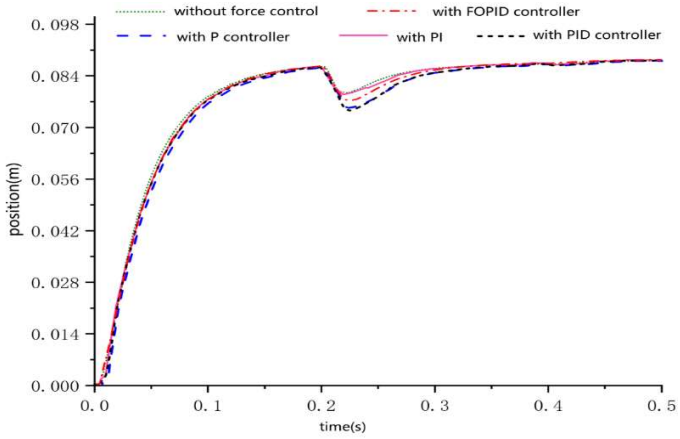

Figure 11. Position response curves under different controllers

3.3.2 Verification of Triangular Wave Dynamic Response

In order to better verify the dynamic response performance of the force equalization controller, the system is set to perform maximum forward and reverse reciprocating deflection motion at the maximum deflection rate of the rudder surface. The position command is in the form of a triangular wave deflection command with an amplitude of 20 ° and T=5s, with the maximum aerodynamic hinge torque load [23], and torque white noise disturbance is added. Under this operating condition, the control effects of force equalization, PID force equalization method, and FOPID method are compared.

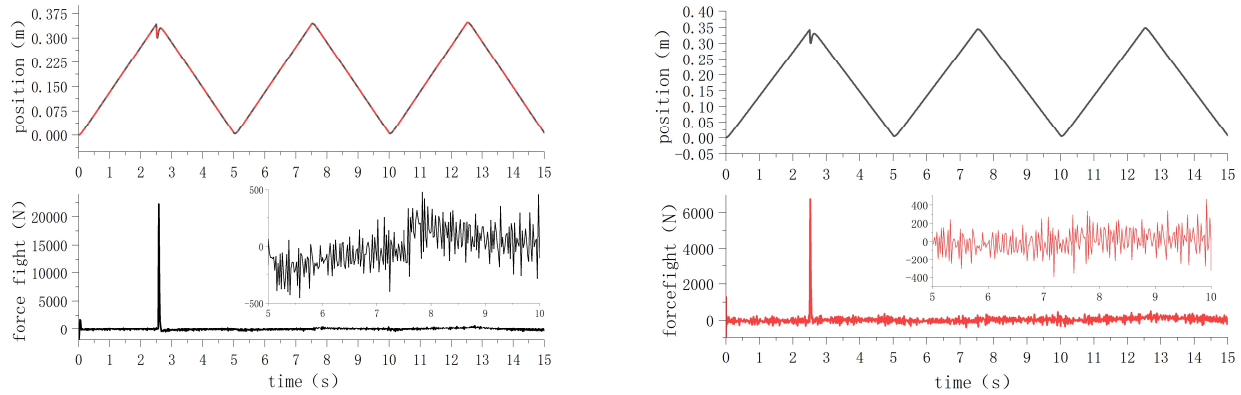

(a)Response with PID force equalization (b) Response with FOPID force equalization

Figure 12. Response with different force equalization strategy

The system response under the PID force balancing method and FOPID force balancing method is shown in Figures 12. The improvement of control effect is divided by the difference between the force fight value under PID strategy and the force fight value under FOPID strategy by the force fight value under PID strategy. Compared with the PID method, FOPID has the following improvements: (1) The maximum force fight under the action of PID and FOPID are 22475.2N and 6954.5N, respectively, which improves the control efficiency of intermittent position signals by 69.06%. (2) The static force fight caused by PID and FOPID are 483.7N and 261.3N, respectively, which improve the control effect of static force fight by about 25.3%. (3) The tracking accuracy of position response is higher.

From the perspective of position response and force fight, the performance of FOPID force equalization controller has significantly improved compared with PID controller.

ISSN: 2414-1895 DOI: 10.6919/ICJE.202412_10(12).0013

4. Conclusion

Aiming to address the issue of force fight existing in the active-active mode operation of dual redundancy EMAs, a fractional order PID control method has been implemented. Force fight and position deviation are established as composite optimization indices, and the optimal parameters for the controller are derived through iterative optimization using a particle swarm optimization algorithm. This approach overcomes the limitations associated with traditional PID parameter tuning methods. The proposed FOPID method has proven to be both effective and feasible, as demonstrated by simulation experiments involving step response and triangular wave response. Compared to the PID force equalization method, the FOPID has more than doubled the control effectiveness in managing both dynamic and static force fight, while also enhancing the speed and accuracy of the system's servo response.

References

[1] CHEN L X.Research on Control Strategy of Electromechanical Actuation Servo System for More Electric Aircraft[D].Xi'an: Northwestern Polytechnical University,2016:4-11.

[2] WEI K P,HU J,YAO J Y,et al. Fast terminal sliding mode control of netrol netwoks for aeromechanical actuators[J].Acta Aeronautica et Astronautica Sinaca,2021, 42(6): 624540.

[3] JIANG X F,HUANG W X,HAO Z Y,et al. Redundant Control System of Dual-Winding Fault-Tolerant Permanent Magnet Motor[J]. TRANSACTIONS OF CHINA ELECTROTECHNICAL SOCIETY, 2015,30(06):22-29.

[4] ARRIOLA D,FRANK THIELECKE.Design of fault-tolerant control functions for a primary flight control system with electromechanical actuators[C].Piscataway, USA:IEEE,2015

[5] WANG H. Literature Review on Force fights and Control Methods of Redundant Actuator Systems[J]. Aircraft Design,2022,42 (3):35-38.

[6] Carl H . Concepts for position and load control for hybrid actuation in primary flight controls[J]. Aerospace Science and Technology, 2007, 11 (2007) 194–201.

[7] FU Y L,FAN D L,LI Z F. Static force equalization for dissimilar redundant actuator system[J]. Journal of Beijing University of Aeronautics and Astronautics, 2014, 40(011):1492-1499.

[8] Fan D L,Fu Y L,Guo Y Q,et al. Dynamic force equali-zation for dissimilar redundant actuator system[J].Journal of Beijing University of Aeronautics and Astronautics,2015,41 (2) : 234-240

[9] ZHANG Y,YUAN Z H.Control Strategy of Aileron's Force-fight[J].International Journal of Multimedia and Ubiquitous Engineering,2014,Vol.9(No.8):299-310.

[10] Salman, IJAZ, Lin, et al. Fractional order modeling and control of dissimilar redundant actuating system used in large passenger aircraft[J]. Chinese Journal of Aeronautics, 2018, v.31;No.146(05):279-290.

[11] Ijaz S , Hamayun M T , Anwaar H , et al. LPV Modeling and Tracking Control of Dissimilar Redundant Actuation System for Civil Aircraft[J]. International Journal of Control Automation and Systems, 2019. 17(X) :1-11.

[12] XUE Y ,YAO Z Q.A Way to Mitigate Force-Fight Oscillation Based on Pressure and Position Compensation for Fly-by-Wire Flight Control Systems[J]. Transactions of the Japan Society for Aeronautical and Space Sciences, 2020, 63(1):1-7.

[13] Rehman W U,Wang X H,Cheng Y Q et al.Motion synchronization for the SHA/EMA hybrid actuation system by using an optimization algorithm[J]. Automatika, 2021,62:3-4, 503-512.

[14] Bingul Z , Karahan O . Real-time trajectory tracking control of Stewart platform using fractional order fuzzy PID controller optimized by particle swarm algo-rithm[J]. Industrial Robot, 2022(4):49-59.

[15] YANG S Z. Nonlinear modeling and fault analysis of flight control electromechanical actuation system[D].Tian'jin:Civil Aviation University of Chi-na,2018: 9-31(in Chinese).

[16] SUN X Z,HOU D,YANG J Z.Analysis of Mechanism and Sensitivity of Force Fight in Dual Redundant Electromechanical Actuators [J].Acta Aeronautica et Astronautica Sinica, (2022-08-31) [2022-10-14]. http://kns.cnki.net/kcms/detail/11.1929.v.20220831.1749.020.html. doi/10.7527/S1000-6893.2022.27661.

ISSN: 2414-1895 DOI: 10.6919/ICJE.202412_10(12).0013

[17] XUE D Y.Fractional Caculus and Fractional-order Control[M]. Version2018.BeiJing: Science Press,2018:32-70,115-126.

[18] WANG C Y.Study on Fractional Order PID Controller Parameter Tuning Methods and Design[D].Ji'lin: Jilin University,2013:29-38.

[19] Shu H, Tu Q, Jiang C, et al. Global Fast Terminal Sliding Mode Control Based on Fractional Order Differentiation for Angular Position Synchronization Con-trol of PMSM[J]. IEEJ Transactions on Electrical and Electronic Engineering, 2022.

[20] ZHANG J. Study on Dual Cylinder Electro-Hydraulic Postion Synchronization System Based on Compound Fuzzy Control[D]. Harbin:Harbin Institute of Technology, 2016:35-40.

[21] GAO S,WANG L,CHEN C B,et al. An Improved Par-ticle Swarm Optimization Algorithm for Fractional Order PID Parameter Tuning[J]. Control Engineering of China, 2017,24(10):2010-2015.

[22] AMIRREZA M M,WIFOLD K,GUSTAVO K C,et al.FOPID Control with Parameter Optimization for Hydrostatically-Actuated Autonomous Excavators[J]. IEEE Instrumentation & Measurement Magazine, 2021,Volume 24(Issue 2) :109-117.